HAMR^3: An Autonomous 1.7g Ambulatory Robot

Andrew T. Baisch[1], *Student Member, IEEE*, Christian Heimlich[1,3], Michael Karpelson[1], *Student Member, IEEE*, and Robert J. Wood[1,2], *Member, IEEE*

***Abstract*— Here we present an autonomous 1.7g hexapod robot that will become a platform for research on centimeter-scale walking robots. It features six spherical five-bar linkages driven by high energy density piezoelectric actuators and onboard power and control electronics. This robot has achieved autonomous ambulation using an alternating tripod gait at speeds up to 0.9 body lengths per second, making this the smallest and lightest hexapod robot capable of autonomous locomotion.**

I. Introduction

Insect-scale mobile robots have been envisioned for exploration of a variety of hazardous environments, including collapsed buildings or natural disaster sites. A swarm of small-scale robots with embedded sensors would have the capability to access confined spaces and quickly search large areas to assist rescue efforts by locating survivors or detecting hazards such as chemical toxicity and temperature.

With these goals in mind, numerous small-scale walking robots have been developed in prior work. At the centimeter-scale, RoACH [1] (3cm long and 2.4g), dynaRoACH [2] (10cm long and 24g), and DASH [3] (10cm long and 16g) represent the state-of-the-art in small-scale legged locomotion performance. They have demonstrated speeds up to 15 body lengths per second on flat ground, high-speed dynamic turns, scaling small obstacles, and traversing granular media [4].

At the millimeter and milligram scale, silicon-based walking robots have been fabricated using MEMS processes [5], [6]. Systems at this scale have proven the potential benefits such as large relative payload and use of batch fabrication. However, on-board power and effective ambulation have not been achieved in a MEMS-scale device.

Our work focuses on developing a centimeter-scale, sub-2 gram walking platform; larger than those achievable with MEMS fabrication but smaller than DASH and RoACH [7],[8]. The goals of this work include studying the dynamics of locomotion on the insect scale and improving meso-scale design and fabrication techniques. Previous work on the second generation Harvard Ambulatory MicroRobot (HAMR^2) demonstrated successful locomotion of a $2g$, $5.7cm$ hexapod. Composed of piezoelectric actuators and flexure-based transmission linkages, HAMR^2 performed well on flat ground, achieving speeds up to 4 body-lengths per second. However, mobility suffered from tethered power and control.

[1]School of Engineering and Applied Sciences and the [2]Wyss Institute for Biologically Inspired Engineering, Harvard University, Cambridge, MA 02138. [3]École Polytechnique Fédérale de Lausanne (EPFL), Lausanne, Switzerland (contact email: abaisch@seas.harvard.edu).

This work describes the 3rd generation Harvard Ambulatory MicroRobot, HAMR^3: a $1.7g$, $4.7cm$ long, autonomous hexapod robot that will become a platform for future centimeter-scale robotics research (see Fig. 1). This paper details the design, fabrication, and assembly of the robot, including piezoelectric actuators, the onboard high voltage electronics necessary to drive them, flexure-based linkages, and circuit board body.

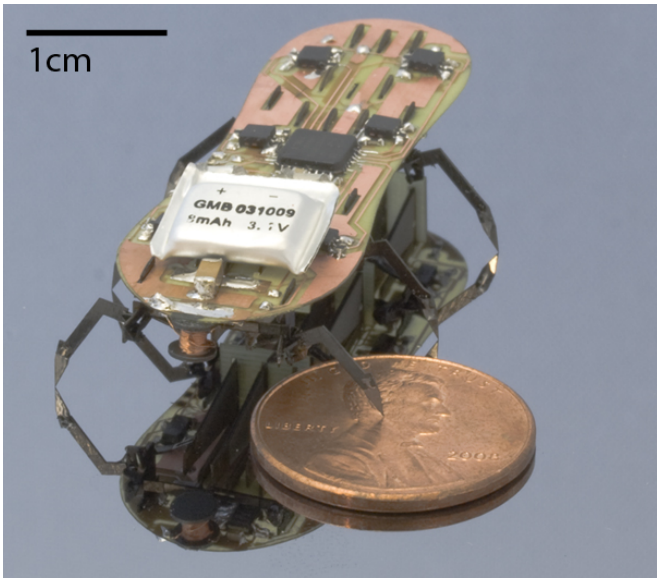

Fig. 1. The third generation Harvard Ambulatory MicroRobot (HAMR^3), a $1.7g$ hexapod robot capable of untethered locomotion.

II. Mechanics

The mechanical design of the HAMR robots have to date been focused on achieving walking gaits by prescribing appropriate outputs at the hip joint. Each hip has been generalized to a two degree of freedom (DOF) spherical five-bar joint with a 'swing' to provide locomotive power in the walking plane and 'lift' to raise the leg off of the walking surface.

Nominally there are twelve total degrees of freedom, which is simplified by a coupling scheme described below. Although the results in Section V describe HAMR^3 walking straight on a flat surface, a goal for future work is to investigate a variety of gaits to enable turning, climbing, and traversing rough terrain. Therefore the actuator coupling scheme remains general enough to accommodate future trials as opposed to only prescribing a single gait. The mechanical

components of HAMR^3, illustrated in Fig. 2, are detailed below.

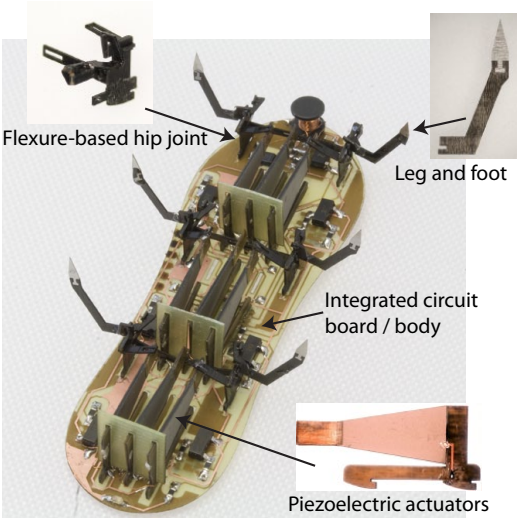

Fig. 2. The mechanical components on HAMR^3. Piezoelectric actuators provide mechanical power through the flexure-based hip joint transmission to drive the legs.

A. Hip joint, legs, and feet

Each leg requires two degrees of freedom for walking: lift and swing. The flexure-based spherical five-bar (SFB) mechanism in Fig. 3, which was introduced in the previous version of HAMR [8], is used to achieve this desired output. The SFB maps two decoupled drive inputs to a single end effector, in this case the leg, through a parallel mechanism that can be idealized as a ball-in socket joint sans axial rotation. Input is taken from two decoupled piezoelectric cantilever actuators through fourbar slider-crank mechanisms to the output. Besides being a simple and compact solution, the SFB enables actuation of two DOFs from two proximally-mounted actuators, thus concentrating mass on the robot body rather than distally as in a serial manipulator.

The SFB is fabricated using the Smart Composite Microstructure (SCM) paradigm [9], which combines rigid carbon fiber links with flexible polyimide joints in a single planar layup. The resulting links may be folded or mechanically interfaced with other parts to form 3D flexure-based mechanical linkages. Each hip joint is fabricated as three planar parts: the two-DOF SFB, swing slider-crank input, and lift slider-crank input. Assembly of each joint requires a mere two folds, followed by mating the three parts using the built-in clip interface (See Fig. 3). The linkages are then fixed to the robot body using a similar clip interface, which is described in Section IV.

The variability in terrain that will be experienced by a walking robot makes *a priori* knowledge of the complete system dynamics impossible. Furthermore, complex feedback on such a small-scale system is a challenge due to the added mass and power requirements for sensors and control electronics. Therefore, a goal of the HAMR project is to investigate the use of passive feedback mechanisms such as

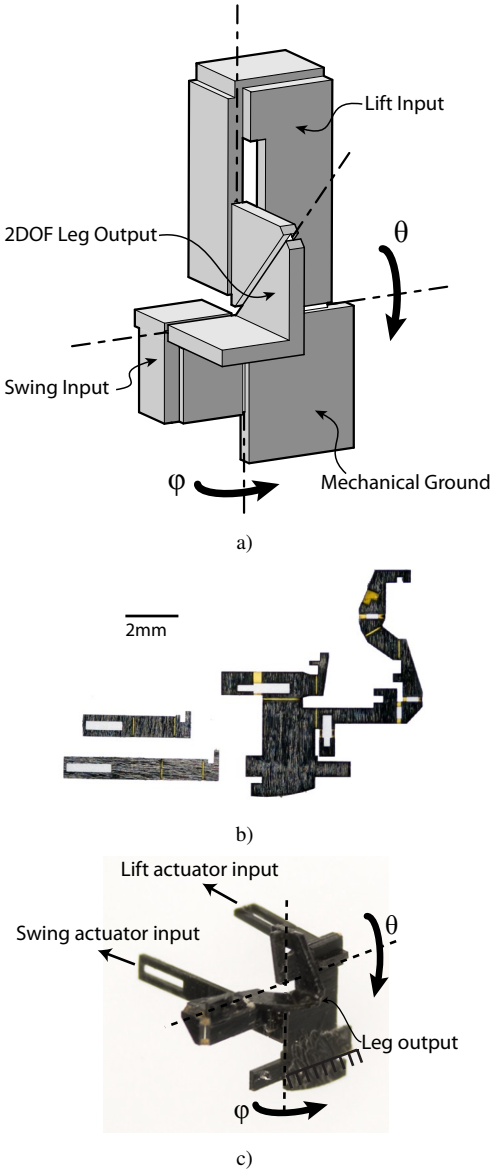

Fig. 3. a) The flexure-based spherical five-bar hip joint for HAMR^3, which provides swing (ϕ) and lift (θ) outputs to the leg. b) The three planar components shown are assembled into c) the complete hip joint linkage.

compliant legs similar to cockroaches [10]. In order to test the effects of varying leg dynamics on performance, the legs are modular. Similarly, the feet are fabricated independently from the leg. Legs and feet are assembled in-plane using mating features, and affixed using a thermoplastic adhesive (Crystalbond^{TM}, Aremco Products, www.aremco.com). Legs were attached to the hip joints using a sliding clip interface and similarly adhered with thermoplastic adhesive. This design will allow future tests on varying leg dynamics and foot attachment mechanisms.

B. Actuation

Consistent with the previous HAMR prototype and other robotic insects [11], optimal energy density piezoelectric bimorph cantilevers [12] are used for actuation on HAMR^3.

These actuators have proven to be suitable for the energy requirements of millimeter-scale mobile robots and have a high bandwidth, enabling quasi-static operation. The optimal energy density design, which consists of a tapered clamped-free cantilever beam, is used to minimize the actuator mass for a desired output (See Fig. 4).

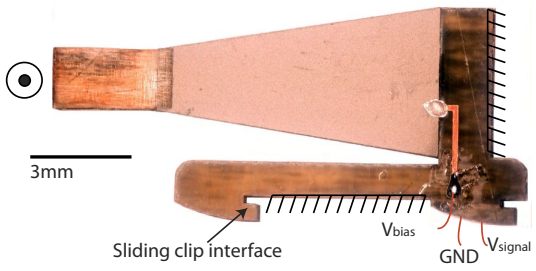

Fig. 4. Optimal energy density piezoelectric bimorph actuators provide mechanical power to the hip joint transmissions on HAMR^3. As shown, the clamped-free cantilever produces motion into and out of the page. The clip interface at the bottom of the actuator creates a simple attachment to the circuit board body, where the three signals are provided from onboard electronics.

The nominal actuator design, composed of a central carbon fiber layer, two $125\mu m$ thick lead-zirconate-titanate (PZT-5H) plates, and electrically-insulating fiberglass tip, was modified from previous versions to include a mechanical clip interface and solderable connections for the three input signals (See Fig. 4). Signals are traced to the PZT plates and central electrode layer using $125\mu m$ copper-clad FR-4 printed circuit board, which additionally provides a rigid mechanical ground at the base of the cantilever.

Nine piezoelectric actuators drive the twelve nominal degrees of freedom on HAMR^3; three actuators are associated with swing, and six with lift. The swing DOFs of each contralateral leg pair are asymmetrically coupled such that driving the actuator left moves the left leg back and the right leg forward and *vice versa*. The lift DOFs are driven using six actuators to satisfy the energy requirements of supporting the robot's mass, as well as to simplify board layout. Individual leg lift control enables a large variety gaits for future testing, however in this version of HAMR, lift actuators share input signals to reduce complexity of the required electronics. Here, each contralateral pair of lift DOFs are also coupled asymmetrically by sharing a drive signal and inverting the actuator's bias and ground.

III. Electronics

The walking performance of the previous HAMR prototype suffered from the use of external electronics (see Fig. 5a). In order to achieve autonomy, onboard electronics must provide the following functions for a robot with up to nine piezoelectric actuators: power conditioning, boost conversion, gait timing, sensor processing, and programming interface. Fig. 5b shows the newly developed autonomous version with all of the onboard electronics.

Commercially available control boards for microrobots, e.g. Plantraco's 0.9g Micro 9 receiver, are not suitable for

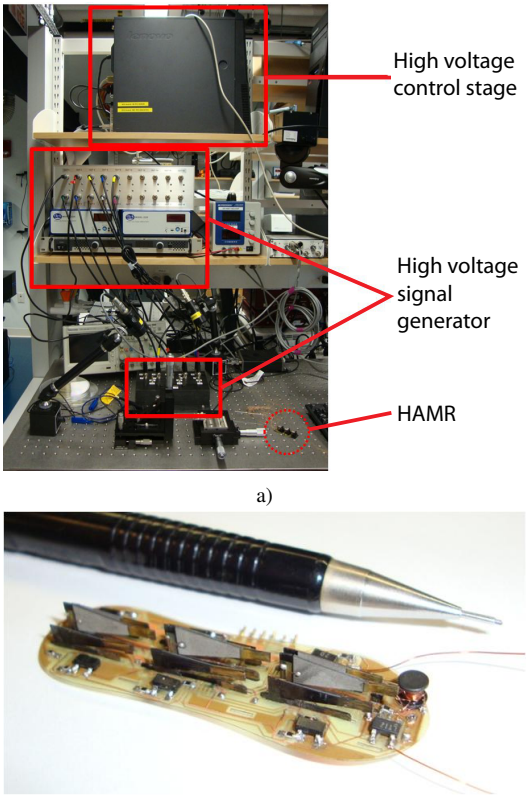

a)

b)

Fig. 5. External power and control setup used for HAMR^2 (top) with the HAMR^2 robot circled. The onboard electronics for the HAMR^3 prototype is shown in the bottom image.

our ultra-lightweight multi-actuator high voltage application, therefore a custom solution is used. Small-scale high voltage drive circuits for bimorph piezoelectric actuators are discussed in [13], [14] and [15]. The circuits described here are derived from those in [13], however energy recovery has been sacrificed to simplify design. This version uses mostly off-the-shelf components and a single microcontroller for the control of the entire robot.

A. Design

The overall approach is shown in Fig. 6a: a low voltage power source is converted into a high voltage drive signal to drive multiple piezoelectric actuators. The actuator motion is mechanically transmitted to the legs to drive the robot forward and sensors send information about the robot's environment (e.g. obstacles) back to the microcontroller to adapt its behavior (turning, stopping, reversing, etc.).

Bimorph piezoelectric actuators can be driven in different ways; [13] gives an overview of the different options. The choice of the drive method depends mainly on the number and type of actuators for a given system. In our multi-actuator case (nine actuators), the simultaneous drive method is used, sharing the high voltage bias among the bimorph actuators. A two-stage design with one voltage conversion stage for all actuators and one driving stage for each of the nine individual actuators has been developed. The different components can

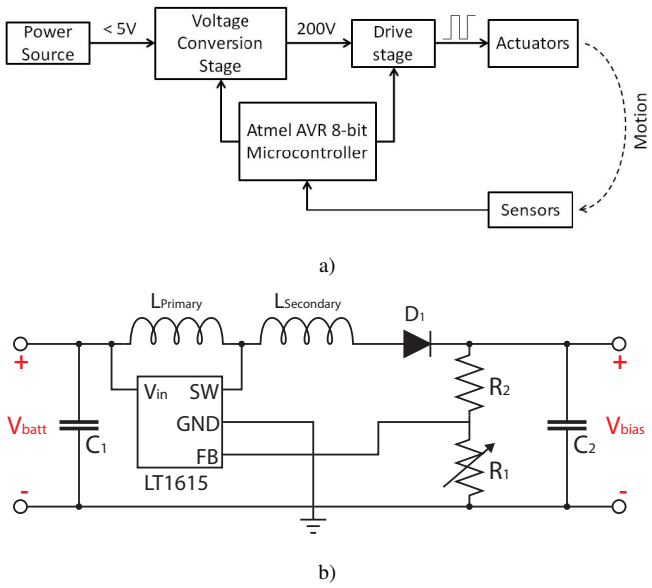

Fig. 6. a) Schematic of the onboard circuitry for HAMR^3, taking low voltage ($< 5V$) input, boosting to the high voltage ($200V$) output to drive piezoelectric actuators. b) Detailed schematic of the high voltage conversion stage.

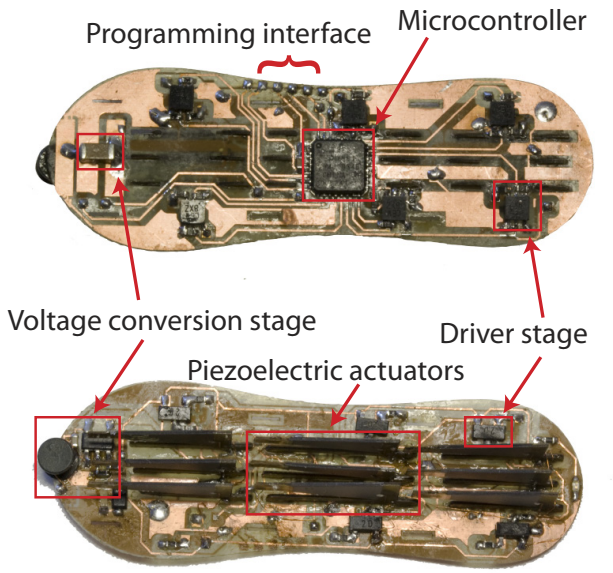

Fig. 7. Diagram of the double-sided circuit required to drive piezoelectric actuators from an onboard power supply on HAMR^3.

be seen in Fig. 7.

a) Voltage conversion stage: Given the desire to operate the actuators at maximum work output (approximately $1-2V/\mu m$ for these materials), and the $127\mu m$ thickness of the available piezoelectric plates, the first stage must produce an output of approximately $200V$. Most compact energy sources suitable for microrobotic applications (lithium batteries, supercapacitors, solar cells, fuel cells) generate low output voltages, ranging typically from 1.5V to 3.7V. Connecting many of such cells in series is not desirable since the packaging overhead causes a significant increase in weight and a considerable reduction in energy density. Therefore, voltage conversion circuits with high step-up ratios, typically from 50 to 100, need to be developed.

Many of the existing circuit topologies are difficult to miniaturize and/or suffer from poor efficiency at the low output power levels typical in small-scale robots. Careful selection and optimization of the conversion circuit is necessary to avoid unnecessarily compromising the system's performance with heavy, inefficient electronics [13].

Here we use a tapped inductor boost converter (Fig. 6b), chosen over alternatives such as charge pumps because of scale, minimal component count and high energy density. With the exception of the step-up transformer, all components are available off-the-shelf; the transformer is custom wound. Given the low input voltage and the desired high output voltage, practical tests have shown that the primary winding should have at least 20 turns with an inductance of $10\mu H$ or more. Best results were achieved with coils having approximately the following characteristics:

- Turn ratio $N = 11$
- Windings: $N_1 = 30$, $N_2 = 330$
- Primary: $L_1 = 13\mu H$, $R_1 = 0.75\Omega$
- Secondary: $L_2 = 1.7mH$, $R_2 = 95\Omega$

The quality of the transformer is influenced by the quality of the hand-made coil. Therefore, in-depth characterization of the transformer is the subject of ongoing research.

b) Drive stage: The drive stage creates a time-varying command signal from the high voltage bias using two transistors. The command signal can be of any form: square, triangular, sinusoidal, etc., depending on the desired output behavior of the actuator. In our case, to maximize joint torque during each step, a ramped square wave is used to drive the piezoelectric actuators. The ramp is introduced to drive the actuator gently to prevent mechanical failure. The ramp is achieved by filtering a binary output from the microcontroller using a resister and the capacitance of the actuator.

c) Microcontroller: A microcontroller small in size, low in power consumption, and with sufficient digital I/O's to drive six actuators (12 signals) and read multiple sensors is required. Atmel's ATtiny861 was found to be a good match for this application.

d) Power source: To power the robot, a compact, lightweight and high energy density power source is needed. Suitable power sources for small-scale robots include ion batteries, supercapacitors, solar cells and fuel cells. Here we use a rechargeable Lithium-Polymer battery, due to off-the-shelf solutions (form, geometry, capacitance), high operating voltage ($3.7V$), high energy density, and high discharge rates. The smallest known available battery is PowerStream's $8mAh$ GM300910 battery (www.powerstream.com), offering a compromise between mass ($330mg$) and runtime. Using this battery, runtimes of over 2 minutes at actuation frequencies of $20Hz$ could be achieved.

B. Body fabrication

To reduce the number of necessary components, a circuit board is used for the robot's body on which all the mechanics, electronics and actuators are installed. A $150\mu m$ thick printed circuit board is used for this purpose, resulting in a weight of about $250mg$ unpopulated. The circuit complexity requires a double-sided board, and a laser-based fabrication method has been developed to create circuit boards in-house. The circuit pattern is created using laser ablation of the resist layer and chemical etching; the vias are created by wire-connection through laser-cut holes. Via fabrication techniques such as plating, immersion, or electrochemical migration are the subject of ongoing work.

C. Results

One voltage conversion stage, one microcontroller, and six drive stages were installed and distributed over the robot to create the necessary drive signals in close proximity to the corresponding actuators. Components were installed on both sides of the board to reduce the necessary surface area (see Fig. 7). Nine piezoelectric bimorph actuators were installed (3 swing and 6 lift), however using the coupling scheme described in Section II-B only six independent drive signals are generated.

To filter the bias voltage, two high voltage capacitors of different size were tested ($0.1\mu F$ and $1\mu F$). The size of the high voltage capacitor has a large influence on the quality of the output voltage but it also significantly increases the mass of the robot ($30mg$ for a $0.1\mu F$ capacitor vs. $300mg$ for a $1\mu F$). In both cases, the boost conversion stage manages to recover rapidly from the voltage drops. Tests with a $0.1\mu F$ vs. a $1\mu F$ capacitor did not show noticeable differences in the robot's behavior.

IV. Assembly

In previous versions of HAMR, integration of mechanics and electronics required a high degree of skill. To generate a working HAMR^3 prototype with onboard electronics, all components were integrated onto a single circuit board that simultaneously acts as a common mechanical ground. Experience with the previous versions also dictated that failure of individual components was common, and therefore modularity was a key component of the system integration concept. A modular design also facilitated rapid parametric testing of linkages and actuators.

The double-sided circuit board, the fabrication of which is detailed in Section III, includes bond pads for surface mount electrical components and cutouts for plug-in mechanics. The full robot assembly began by populating the circuit board with all surface mount components, and concluded with manual placement of actuators and linkages into their correct slot. Mechanics are fixed by sliding them backwards to engage them with the board using a simple clip mechanism (See Fig. 3 and Fig 4), assisting in alignment as well as providing a press-fit interface. Linkages were locked in place using Crystalbond^{TM}, while actuators were fixed to their appropriate bond pads with solder. The current assembly process takes several hours to complete, an improvement from days for the previous HAMR prototypes. Although manual soldering was used in this work, the assembly method was designed to use reflow in the future for single-step assembly.

TABLE I
Mass distibution of all HAMR^3 components

Component	Mass (mg)
Unpopulated circuit board	250
Electronic components	500
Battery	330
Actuators	$9\times 65 = 585$
Hip joint transmissions	$6\times 8 = 48$
Legs and feet	$6\times 3 = 18$
Total mass	1730

V. Locomotion Performance

The completed HAMR^3 prototype is $1.7g$ and $48mm$ long and demonstrates untethered walking on flat ground. Table I is a summary of the mass of each component. A number of ground surfaces were tested for walking, however card stock was chosen for initial performance tests since it provided relatively consistent results; interaction with many surfaces exhibited slipping or sticking, which slowed or prohibited locomotion. The legs and feet chosen for these trials were rigid 6-ply carbon fiber laminate and stainless steel points, respectively.

Walking speed performance was characterized using the alternating tripod gait at actuator frequencies from $1-30Hz$, the results of which are summarized in Fig. 9. Fig. 8 shows the robot walking on flat ground using $15Hz$ gait frequency, and other speeds are shown in the supplemental video. The optimal frequency for the chosen foot and ground conditions was found at $20Hz$, where HAMR walked on average $3cm/s$ (0.625 body lengths per second) and hit a maximum speed of $4.3cm/s$ (0.9 body lengths per second) during one trial. Beyond this frequency the robot exhibited a drop in speed due in part to a loss of ground contact (slipping) during the leg stroke as well as instability in the walking plane. The latter is best evidenced by the performance at $30Hz$, at which the robot traveled straight at $3cm/s$ for a mere $2cm$ before turning 180° to the left.

The walking performance of HAMR^3 is limited by design flaws in flexure compliance, actuator output, and weight distribution. Examining walking at $1Hz$ from the side (see the supplemental video), shows the primary effect is that the rear legs drag, rather than lift off the ground during their swing phase. It was witnessed that this is further exacerbated at lower frequencies as the legs slip away from the body, effectively increasing the friction force of the legs dragging on the ground. At these lower frequencies, velocity was recorded up to 40% greater in the first $1cm$ of travel than at the recorded steady state values in Fig. 9. This behavior also prohibited more advanced maneuvers such as walking up inclines or in reverse.

To test the feasibility of prolonged missions, system life was tested for a full battery charge. With the $8mAHr$ battery,

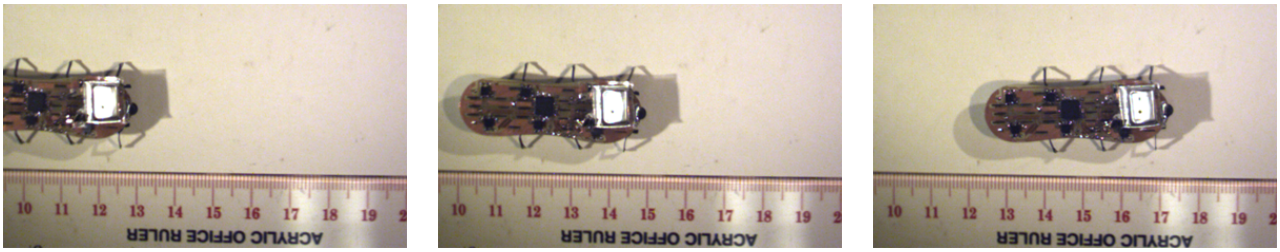

t=0s t=1s t=2s

Fig. 8. Untethered walking of HAMR^3 at $15Hz$ gait frequency using the alternating tripod gait.

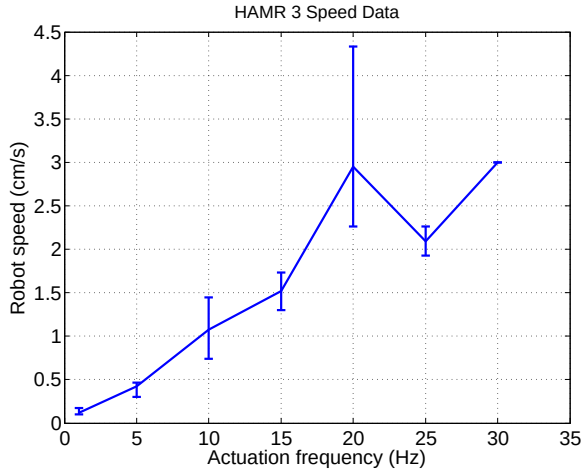

Fig. 9. Speed trial results for 1-30Hz actuator frequency. Up to 25Hz actuator frequency, values are the mean steady state velocity and error bars represent the maximum and minimum trial values. Above 25Hz, the robot failed to follow a straight line and speed results were taken from the first $2cm$ of travel.

HAMR^3 walked on flat ground for 2-2.5 minutes at $20Hz$ actuator frequency ($360-450cm$). Testing a larger, $45mAHr$ battery, the system worked in air for 30 minutes. The larger battery, which increased total mass by $500mg$ also shows that HAMR^3 can carry some payload; under this condition the robot was still capable of forward locomotion, albeit slower than the lighter version. This demonstrates that the inclusion of additional components such as sensors is feasible with the current design.

VI. Discussion and Future Work

The complete design and results of the third generation Harvard Ambulatory MicroRobot, which is capable of untethered locomotion on flat terrain, has been presented. The work here focused on small-scale electronics to drive piezoelectric actuators up to $200V$, the improvement of mechanical components over previous work [8], and integration of mechanics and electronics onto a single custom circuit board. The results of the first prototype of this design are a $1.7g$ and $47mm$ long robot, which to our knowledge is the smallest and lightest autonomous hexapod robot. Despite the limitations mentioned in Section V, HAMR^3 proves the capability to create an autonomous insect-scale walking robot using the selected piezoelectric actuation and SCM fabrication technologies and is therefore a platform for further work towards a fully-autonomous version with increased maneuverability.

Future work on the mechanics will address the design flaws mentioned in Section V to create a robot capable of locomotion on a variety of terrains. Once such mechanical issues are solved, HAMR will be a platform for future research in the following areas:

- Testing a variety of gaits for walking, turning, and climbing, by varying actuator drive signals and phase offsets between legs.
- Implementing feedback control, including onboard sensors for trajectory following and obstacle avoidance. Furthermore, HAMR will be a platform for testing biologically-inspired sensors such as optical flow and [16] and antennae for wall following [17].
- Varying leg dynamics by implementing passive mechanical elements to enable gait stabilization without proprioception, similar to most natural ambulation [10].
- Foot attachment mechanisms will be studied with the hope of obtaining ideal foot-ground contact on flat ground and while climbing. A primary focus will be implementing existing solutions found in larger climbing robots, such as gecko-inspired adhesives for smooth surfaces [18], [19] and tarsal claws for rough terrain [20].

VII. Acknowledgements

The authors gratefully acknowledge the National Science Foundation (award number IIS-0811571) and the Wyss institute for Biologically-Inspired Engineering (Harvard University) for support of this work. Any opinions, findings, and conclusions or recommendations expressed in this material are those of the authors and do not necessarily reflect the views of the National Science Foundation. Andrew Baisch was supported by the Department of Defense (DoD) through the National Defense Science & Engineering Graduate Fellowship (NDSEG) Program.

References

[1] A. Hoover, E. Steltz, and R. Fearing, "Roach: An autonomous 2.4 g crawling hexapod robot," in *IEEE/RSJ Intl. Conf. on Intelligent Robots and Systems*.

[2] A. Hoover, S. Burden, X.-Y. Fu, S. Sastry, and R. Fearing, "Bio-inspired design and dynamic maneuverability of a minimally actuated six-legged robot," in *IEEE Intl. Conf. on Robotics and Biomimetics*, Tokyo, Japan, Sept. 2010.

[3] P. Birkmeyer, K. Peterson, and R. Fearing, "DASH: A dynamic 16g hexapedal robot," in *IEEE/RSJ Intl. Conf. on Intelligent Robots and Systems*, St. Louis, MO, 2009, pp. 2683–2689.
[4] C. Li, A. Hoover, P. Birkmeyer, P. Umbanhowar, R. Fearing, and D. Goldman, "Systematic study of the performance of small robots on controlled laboratory substrates," in *SPIE Defense, Security, and Sensing Conf.*, Orlando, FL, Apr. 2010.
[5] S. Hollar, A. Flynn, C. Bellew, and K. Pister, "Solar powered 10*mg* silicon robot," in *IEEE Intl. Conf. on Micro Electro Mechanical Systems*, Kyoto, Japan, Jan. 2003.
[6] T. Ebefors, J. Mattsson, E. Kälvesten, and G. Stemme, "A walking silicon micro-robot," in *10th Intl. Conf. on Solid-State Sensors and Actuators*, Sendai, Japan, June 1999, pp. 1202–1205.
[7] A. Baisch and R. Wood, "Design and fabrication of the harvard ambulatory microrobot," in *14th Intl. Symp. on Robotics Research*, Lucerne, Switzerland, Sept. 2009.
[8] A. Baisch, P. Sreetharan, and R. Wood, "Biologically-inspired locomotion of a 2g hexapod robot," in *IEEE/RSJ Intl. Conf. on Intelligent Robots and Systems*, Taipei, Taiwan, 2010, pp. 5360–5365.
[9] R. Wood, S. Avadhanula, R. Sahai, E. Steltz, and R. Fearing, "Microrobot design using fiber reinforced composites," *J. of Mechanical Design*, vol. 130, no. 5, May 2008.
[10] S. Sponberg and R. Full, "Neuromechanical response of musculoskeletal structures in cockroaches during rapid running on rough terrain," *J. of Experimental Biology*, vol. 211, pp. 433–446, May 2008.
[11] R. Wood, "The first flight of a biologically-inspired at-scale robotic insect," *IEEE Transactions on Robotics*, vol. 24, no. 2, Apr. 2008.
[12] R. Wood, E. Steltz, and R. Fearing, "Optimal energy density piezoelectric bending actuators," *J. of Sensors and Actuators A: Physical*, vol. 119, no. 2, pp. 476–488, 2005.
[13] M. Karpelson, G. Wei, and R. Wood, "Milligram-scale high-voltage power electronics for piezoelectric microrobots," in *IEEE Intl. Conf. on Robotics and Automation*, Kobe, Japan, 2009, pp. 2217–2224.
[14] R. Wood, S. Avadhanula, E. Steltz, M. Seeman, J. Entwistle, A. Bacharach, G. Barrows, S. Sanders, and R. Fearing, "Design, fabrication and initial results of a 2g autonomous glider," in *Conf. of IEEE Industrial Electronics Society*, Raleigh, NC, Nov. 2005.
[15] R. Sahai, S. Avadhanula, R. Groff, E. Steltz, R. Wood, and R. Fearing, "Towards a 3g crawling robot through the integration of microrobot technologies," in *IEEE Intl. Conf. on Robotics and Automation*, Orlando, FL, May 2006.
[16] G. Barrows and C. Neely, "Mixed-mode VLSI optic flow sensors for in-flight control of a micro air vehicle," *SPIE Critical Technologies for the Future of Computing*, vol. 4109, pp. 52–63, 2000.
[17] A. Lamperski, O. Loh, B. Kutscher, and N. Cowan, "Dynamical wall following for a wheeled robot using a passive tactile sensor," in *IEEE Intl. Conf. on Robotics and Automation*, Barcelona, Spain, 2005, pp. 3838–3843.
[18] S. Kim, M. Spenko, S. Trujillo, D. Santos, and M. Cutkosky, "Smooth vertical surface climbing with directional adhesion," *IEEE Transactions on Robotics*, vol. 24, pp. 65–74, Feb. 2008.
[19] M. Murphy, C. Kute, Y. Menguc, and M. Sitti, "Waalbot II: Adhesion Recovery and Improved Performance of a Climbing Robot using Fibrillar Adhesives," *The Intl. J. of Robotics Research*, vol. 30, no. 1, p. 118, 2011.
[20] A. Asbeck, S. Kim, M. Cutkosky, W. Provancher, and M. Lanzetta, "Scaling hard vertical surfaces with compliant microspine arrays," *The Intl. J. of Robotics Research*, vol. 25, no. 12, p. 1165, 2006.